

# Exploring the Cosmic Web in the Sloan Digital Sky Survey Data Release Seven using the Local Dimension.

Prakash Sarkar<sup>1\*</sup>, Biswajit Pandey<sup>2,4†</sup>, Somnath Bharadwaj<sup>3‡</sup>

<sup>1</sup>*IUCAA, Pune University Campus, Post Bag 4, Ganeshkhind, Pune 411 007, India.*

<sup>2</sup>*Max-Planck Institute for Astrophysics, Karl-Schwarzschild Str. 1, D85748, Garching, Germany*

<sup>3</sup>*Department of Physics and Meteorology & Centre for Theoretical Studies, IIT Kharagpur, 721 302, India*

<sup>4</sup>*Department of Physics, Visva-Bharati University, Santiniketan, Birbhum, 731235, India*

22 January 2013

## ABSTRACT

It is possible to visualize the Cosmic Web as an interconnected network of one-dimensional filaments, two-dimensional sheets and three-dimensional volume-filling structures which we refer to as clusters. We have used the Local Dimension  $D$ , which takes values  $D = 1, 2$  and  $3$  for filaments, sheets and clusters, respectively, to analyse the Cosmic Web in a three-dimensional volume-limited galaxy sample from the Sloan Digital Sky Survey Data Release 7. The analysis was carried out separately using three different ranges of length-scales:  $0.5$ - $5$ ,  $1$ - $10$  and  $5$ - $50 h^{-1}\text{Mpc}$ . We find that there is a progressive increase in the  $D$  values as we move to larger length-scales. At the smallest length-scale, the galaxies predominantly reside in filaments and sheets. There is a shift from filaments to sheets and clusters at larger scales. Filaments are completely absent at the largest length-scale ( $550 h^{-1}\text{Mpc}$ ). Considering the effect of the density environment on the Cosmic Web, we find that the filaments preferentially inhabit regions with a lower density environment as compared to sheets and clusters which prefer relatively higher density environments. A similar length-scale dependence and environment dependence was also found in a galaxy sample drawn from the Millennium Simulation which was analysed in exactly the same way as the actual data.

**Key words:** methods: data analysis - galaxies: statistics - large-scale structure of Universe

## 1 INTRODUCTION

Galaxy redshift surveys provide us with a picture of the large scale structures in the present day universe. All the major galaxy redshift surveys like the Center for Astrophysics (CfA) Survey (Geller & Huchra, 1989), the Las Campanas Redshift Survey (LCRS) (Shectman et al., 1996), the Two-Degree Field Galaxy Redshift Survey (2dFGRS) (Colless et al. 2001) and the Sloan Digital Sky Survey (SDSS) (York et al. 2000) clearly show that the galaxies are distributed in a complex interconnected network of filaments, sheets and clusters encircling nearly empty voids. This interconnected network is often referred to as the “Cosmic Web” (Bond et al., 1996). Quantifying the Cosmic Web and understanding its origin is one of the most interesting and challenging issues in cosmology.

A wide variety of statistical measures have so far been employed to quantify the Cosmic Web. The void probability function (White, 1979), the percolation analysis (Shandarin & Zeldovich, 1983) and the genus curve (Gott, Mellot & Dickinson, 1986) are some of the earliest statistics introduced to quantify the topology of the galaxy distribution. The Minkowski functionals (Mecke et al., 1994) provide a global characterization of structures. Ratios of the Minkowski functionals can be used to define the ‘Shapefinders’ which are a set of shape diagnostics for both simple and topologically complex objects (Sahni et al. 1998). Bharadwaj et al. (2000) have introduced a two dimensional (2D) version of Shapefinders. There are quite a few different techniques that have been introduced to identify voids in the galaxy distribution (El-Ad & Piran, 1997; Hoyle & Vogeley, 2002; Platen et al., 2007; Neyrinck, 2008). Stoica et al. (2007) have proposed a three dimensional object point process to delineate filaments in the large scale structures. Colombi, Pogosyan & Souradeep (2000) have proposed a Hessian based statistics to study the topology of excursion sets at the percolation threshold. The Smoothed Hessian Major Axis Filament Finder (SHMAFF) (Bond et al. 2010) has been introduced to identify filaments, sheets and clusters in the galaxy distribution. Aragón-Calvo et al. (2007) have introduced a multiscale morphology filter to automatically segment the cosmic structures into its basic components namely clusters, filaments and walls. Sousbie et al. (2008) have proposed a skeleton formalism to quantify filamentary structures in a three dimensional density field. Aragon-Calvo et al. (2008) have introduced the Spine of the Cosmic Web which provides a complete framework for the identification of different morpho-

\* E-mail:sarkar@iucaa.ernet.in

† Email:biswa@mpa-garching.mpg.de

‡ Email:somnath@phy.iitkgp.ernet.in

logical components of the Cosmic Web. Each of the techniques mentioned above quantifies one or atmost a few aspects of the complex network referred to as the Cosmic Web. A comprehensive quantification of the Cosmic Web is still forthcoming, leaving considerable scope for work in this direction.

The early galaxy redshift surveys like the LCRS probed thin, nearly two dimensional (2D) slices through the universe. Initial investigations (Bharadwaj et al., 2000) which used the 2D Shapefinders show the galaxy distribution in the LCRS to have excess filamentarity in comparison to a random distribution of points. Bharadwaj et al. (2004) show the filamentarity in the LCRS to be statistically significant up to a length-scales of  $70 - 80 h^{-1} \text{ Mpc}$  but not beyond. Longer filaments, though present in the data, were not found to be statistically significant, and were possibly the outcome of chance alignments of shorter filaments. Bharadwaj & Pandey (2004) have used N-body simulations to show that the filamentarity in the LCRS is consistent with the LCDM model with a mild bias. Subsequent work (Pandey & Bharadwaj, 2005) performed a 2D analysis of thin slices from the SDSS. This confirmed the results obtained earlier using the LCRS. It was also found that the distribution of brighter galaxies has a lower connectivity and filamentarity as compared to the fainter ones. The filamentarity was also found to depend on other galaxy properties like colour and morphology (Pandey & Bharadwaj, 2006), and the star formation rate (Pandey & Bharadwaj, 2008). Pandey & Bharadwaj (2007) have computed the filamentarity for galaxy samples in different luminosity bins and compared these to the filamentarity in simulated galaxy samples with different values of the linear bias parameter to obtain a luminosity-bias relation. A recent 2D analysis of the luminous red galaxies in the SDSS shows the filamentarity to be statistically significant to length-scales as large as  $100 \text{ to } 130 h^{-1} \text{ Mpc}$  (Pandey et al., 2011), which are considerably larger than those found earlier in the LCRS and the SDSS main galaxy sample.

Though the Cosmic Web is relatively easy to visualize and analyze in 2D, this has several limitations which can only be overcome in a three dimensional (3D) analysis. For example, a 2D filament could actually be a section through a 3D sheet. Sarkar & Bharadwaj (2009)(henceforth Paper I) have proposed the Local Dimension as a 3D statistics for analysing the Cosmic Web. This can, in principle, be used to classify different structural elements along the Cosmic Web as filaments, sheets and clusters. Tests with cosmological N-body simulations (Paper I) show that the structures identified a filaments by the Local Dimension match quite well with the visual appearance. The structures identified as sheets, however, could not be visually identified. This was attributed to the fact that the visual appearance is determined by the most dominant structures in the field which usually are the filament, whereas the sheets which are relatively diffuse structures

are not visually identified. Paper I also showed that the Local Dimension could also be used to address a variety of issues like determining the relative fraction of galaxies in filaments, sheets and clusters respectively.

In the present work we have used the Local Dimension to analyse the patterns in the galaxy distribution in the Sloan Digital Sky Survey Data Release Seven (SDSS DR7). We have also carried out a similar analysis on a galaxy catalogue from the semi-analytic model of galaxy formation implemented in the Millennium Simulation (Springel et al., 2005), and compared the results from the actual data with those from the simulation. The Local Dimension classifies the different structural elements along the Cosmic Web as filaments, sheets and clusters. We have used this to study the relative fraction of galaxies in these three different kinds of structures. Further, we also study how these three different kinds of structures are distributed with reference to varying density environments. For example, it is possible that the filaments are preferentially distributed in high density environments relative to the low density environments. It is well accepted that the Cosmic Web is a complex network whose morphology and connectivity will depend on the length-scale at which the analysis is carried out. The galaxy distribution is expected to approach homogeneity at large length scales, and it is known (Sarkar et al., 2009) that the SDSS DR6 is consistent with homogeneity at length-scales beyond  $60 - 70 h^{-1} \text{ Mpc}$ . Given these considerations, we have carried out the entire analysis for three different ranges of length-scales namely  $0.5$  to  $5 h^{-1} \text{ Mpc}$ ,  $1$  to  $10 h^{-1} \text{ Mpc}$  and  $5$  to  $50 h^{-1} \text{ Mpc}$ .

An brief outline of the paper follows. In Section 2 we describe the Local Dimension which is the method that we have adopted to analyse the Cosmic Web and in Section 3 we discussed the data and the method of analysis while Section 4 contains the results and conclusions.

## 2 THE LOCAL DIMENSION

The Cosmic Web may be thought of as an interconnected network of different structural elements. Any particular structural element may be classified as being either a cluster, a filament or a sheet. The Local Dimension, introduced in Paper I, is a simple yet effective method to quantify the shape of individual structural elements along the Cosmic Web. The entire analysis is based on the following argument. Consider, for example, a galaxy ‘G’ located in a filament which is, by definition, a one dimensional structure. We expect  $N(< R)$ , the number of other galaxies within a sphere of comoving radius  $R$  centered on ‘G’, to scale as  $N(< R) = AR$ . Similarly, we expect a scaling  $N(< R) = AR^D$  with  $D = 2$  and  $3$  if  $G$  were located in a sheet and a cluster respectively.

The exponent  $D$  quantifies the dimension of the galaxy distribution in the neighbourhood of  $G$ , and hence we refer to it as the Local Dimension. In principle the Local Dimension provides a technique to determine whether a galaxy is located in a filament, a sheet or a cluster.

Consider, for example, a part of the Cosmic Web where there is a filament connected to a sheet (Figure 1 of Paper 1). We expect  $D = 1$  and  $2$  for the galaxies located in the filament and the sheet respectively. We also expect that the galaxies located near the junction of the two structures will not exhibit a well defined scaling behaviour, and it will therefore not be possible to determine the Local Dimension  $D$  for these galaxies. In a typical situation where the Cosmic Web is a complex, interconnected network of different kinds of structural elements only a fraction of all the galaxies in the entire survey will have a definite value of the Local Dimension  $D$ .

We have, until now, not taken into account the fact that galaxies are discrete objects with finite, non-zero intergalactic separations. It is thus necessary to consider a finite range of comoving length scales  $R \leq R_2$  in order to determine if there is a scaling behaviour  $N(< R) = AR^D$  and thereby estimate the Local Dimension  $D$ . Contrast this with a continuum where it is possible to study the scaling behaviour in the limit  $R \rightarrow 0$  and it is not necessary to refer to a finite range of length-scales. Further, the Cosmic Web is expected to look different when viewed at different length-scales. We also expect the Cosmic Web to approach a homogeneous network beyond length-scales of  $60 - 70 h^{-1} \text{ Mpc}$  (Sarkar et al., 2009) where the galaxy distribution is known to approach homogeneity. It is thus interesting and useful to separately analyze the scaling behaviour across different ranges of length-scale. Based on this we also introduce a lower length-scale  $R_1$  and study the scaling behaviour over different ranges of length-scales  $R_1 \leq R \leq R_2$ .

The values of Local Dimensions once determined, by fitting power law over the length-scales  $R_1 \leq R \leq R_2$ , can be put to use to address a variety of issues. First, we can identify individual structures like filaments or sheets. The relative abundance of different  $D$  values allows us to estimate the fraction of galaxies that reside in sheets, filaments and clusters respectively. The spatial distribution of the  $D$  values allowed us to study how the different kinds of structural elements are interconnected or “woven into the Cosmic Web”.

### 3 DATA AND METHOD OF ANALYSIS

#### 3.1 SDSS DR7 Data

Our present analysis is based on galaxy redshift data from the SDSS DR7 (Abazajian et al., 2009). The SDSS DR7 includes 11,663 square degrees of imaging and 9380 square degrees of spec-

troscopy with 930,000 galaxy redshifts. For the present work we have used the Main Galaxy Sample for which the target selection algorithm is detailed in Strauss et al. (2002). The Main Galaxy Sample comprises of galaxies brighter than a limiting r band Petrosian magnitude 17.77. The data was downloaded from the Catalog Archive Server (CAS) of SDSS DR7 using a Structured Query Language (SQL) search. We have identified a contiguous region in the Northern Galactic Cap which spans  $-40^\circ < \lambda < 33^\circ$  and  $-30^\circ < \eta < 30^\circ$  where  $\lambda$  and  $\eta$  are survey co-ordinates defined in Stoughton et al. (2002). A volume limited galaxy subsample was constructed in this region by restricting the extinction corrected Petrosian r band apparent magnitude to the range  $14.5 \leq m_r \leq 17.77$  and restricting the absolute magnitude to the range  $-19 \leq M_r \leq -20.5$ . This gives us 47705 galaxies in the redshift range  $0.035 \leq z \leq 0.076$  which corresponds to the comoving radial distance range  $104 h^{-1} \leq r \leq 223 h^{-1}$  Mpc. At the redshift  $z = 0.035$ , the comoving volume corresponding to our sub-sample subtends  $124 h^{-1} \text{Mpc} \times 104 h^{-1} \text{Mpc}$  along the transverse directions.

### 3.2 Millennium Data

The Millennium Simulation (Springel et al., 2005) is a large cosmological N-body simulation which traced  $2160^3$  particles from redshift 127 to the present in a periodic comoving box of side  $500 h^{-1} \text{Mpc}$ . We have used a semi-analytic galaxy catalogue generated by Guo et al. (2011) who updated the previously available galaxy formation models (Springel et al. 2005; Croton et al. 2006; De Lucia & Blaizot 2007) with improved versions and implemented galaxy formation models on the Millennium Simulation. Semi-analytic models are simplified simulations of the formation and evolution of galaxies in a hierarchical clustering scenario incorporating all relevant physics of galaxy formation processes. The spectra and magnitude of the model galaxies were computed using population synthesis models of Bruzual & Charlot (2003). Using the peculiar velocities, we map the galaxies to redshift space and then identify a region having the same geometry as our actual data. Applying the same magnitude cuts as those used for the actual data, we have extracted the same number of galaxies as in our final SDSS data and used this in our subsequent analysis.

### 3.3 Method of analysis

We have determined  $N(< R)$  at several  $R$  values for each galaxy in our sample. For each galaxy, its distance from the survey boundary sets the largest value of  $R$  for which it is possible to estimate  $N(< R)$ . We have assigned the Poisson error  $\Delta N(< R) = \sqrt{N(< R)}$  to each measured value

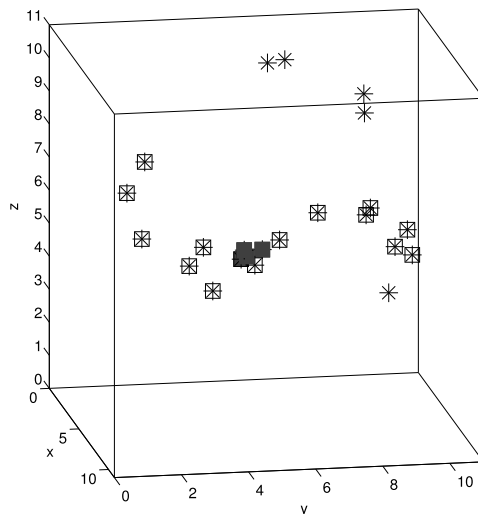


**Figure 1.** The galaxy distribution within  $5 h^{-1}$  Mpc of one of the SDSS DR7 galaxies that was identified to have  $D \approx 1$  across the length-scales  $0.5$  to  $5 h^{-1}$  Mpc. The galaxies are all shown with crosses. We have used a Friend-of-Friend (FoF) algorithm with a linking length of  $\sqrt{3} h^{-1}$  Mpc to highlight any connected structure in the galaxy distribution in this figure. This yields a single filamentary structure containing the majority of the galaxies. All the galaxies belonging to this connected structure are shown with cells. The filled cells represents galaxies with  $D \approx 1$ . It was not possible to determine  $D$  for the other galaxies in this figure.

of  $N(< R)$ . A  $\chi^2$  minimisation procedure was used to determine the best fit power law  $N(< R) = AR^D$  to the  $N(< R)$  measured for each galaxy. The value of  $D$  is accepted as the Local Dimension corresponding to the particular galaxy if the chi-square per degree of freedom of the power law fit satisfies,  $\chi^2/\nu \leq 1$ . The power law fit is rejected for larger values of  $\chi^2/\nu$ , and the Local Dimension is undetermined for these galaxies. The fitting procedure was restricted to values within the range  $R_1 \leq R \leq R_2$  in length-scale.

We have carried out the analysis for three different ranges of length-scales, each covering a decade. Values of  $D$  were determined separately across the length-scales  $0.5$  to  $5 h^{-1}$  Mpc,  $1$  to  $10 h^{-1}$  Mpc and  $5$  to  $50 h^{-1}$  Mpc. It was possible to determine a definite value of  $D$  for 3484, 9082 and 288 galaxies at the three respective ranges of length-scale mentioned above.

In order to illustrate our method of classifying cosmological structures we show the galaxy distribution in the vicinity of one of the SDSS galaxies that was identified to have  $D \approx 1$  across the length-scales  $0.5$  to  $5 h^{-1}$  Mpc (Figure 1). The expected filament is clearly visible passing through the center of the figure. We note that there are several galaxies with  $D = 1$  arranged along the filament visible in the figure. Figure 2 shows a similar plot for one of the galaxies with  $D \approx 1$  from the Millennium data.

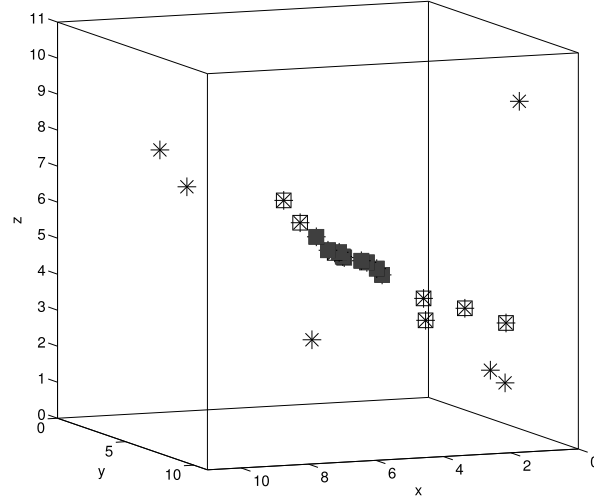


**Figure 2.** Same as Figure 1, for one of the galaxies with  $D \approx 1$  from the Millennium Data.

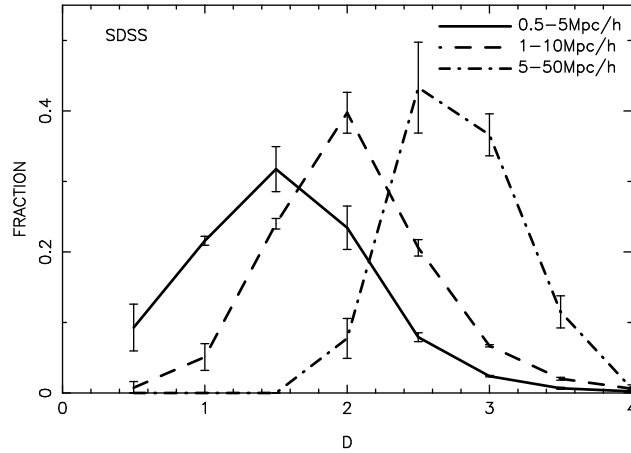


**Figure 3.** This shows the fraction of galaxies with a particular  $D$  value for the SDSS data. The three different curves correspond to  $D$  values that were determined using the length-scales  $0.5 - 5 h^{-1} \text{ Mpc}$ ,  $1 - 10 h^{-1} \text{ Mpc}$  and  $5 - 50 h^{-1} \text{ Mpc}$  respectively. The bins in  $D$  have size  $\pm 0.25$ .

## 4 RESULTS AND CONCLUSIONS

### 4.1 Distribution of $D$ values

We first analyse the fraction of centers with different  $D$  values, shown in Figure 3. The  $D$  values were divided into bins of width  $\pm 0.25$ . The error bars in the data have been estimated using bootstrap re-sampling of the data. Ten bootstrap samples were used for this purpose.

The solid curve in Figure 3, which corresponds to the results for  $0.5$  to  $5 h^{-1} \text{ Mpc}$ , shows a broad peak with a maxima at  $D = 1.5$ . The bin centered at  $D = 2$  contains the second largest fraction of galaxies. These two bins together contain more than 50% of the centers for which  $D$  could be determined. This value indicates that the galaxies in the Cosmic Web are predominantly contained in sheets and filaments at the length-scales  $0.5$  to  $5 h^{-1} \text{ Mpc}$ , with the sheets being somewhat more dominant than the filaments. The dashed curve in Figure 3, which corresponds



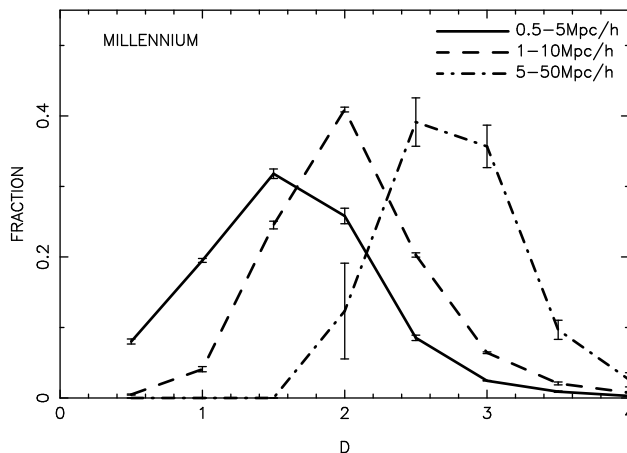


**Figure 4.** This shows the fraction of galaxies with a particular  $D$  value for the data from the Millennium simulation. The three different curves correspond to  $D$  values that were determined using the length-scales  $0.5 - 5 h^{-1} \text{ Mpc}$ ,  $1 - 10 h^{-1} \text{ Mpc}$  and  $5 - 50 h^{-1} \text{ Mpc}$  respectively. The bins in  $D$  have size  $\pm 0.25$ .

to length-scales  $1$  to  $10 h^{-1} \text{ Mpc}$ , shows a sharp peak at  $D = 2$ . The fraction of galaxies in the neighbouring bins ( $D = 1.5$  and  $2.5$ ) falls to nearly half the fraction in this bin. The three bins at  $D = 1.5$ ,  $2$  and  $2.5$  together contains more than 80% of the centers for which  $D$  could be determined. This indicates that the galaxies in the Cosmic Web are predominantly in sheets over the length-scale  $1$  to  $10 h^{-1} \text{ Mpc}$ . The dot-dashed curve in Figure 3, which corresponds to the length-scales  $5$  to  $50 h^{-1} \text{ Mpc}$ , peaks at  $D = 2.5$  and  $D = 3$ . The  $D = 2.5$  contains the maximum no of centers. The two bins combinely contains more than 70% of the centers. This indicates that the galaxies in the Cosmic Web are predominantly in sheets and clusters (volume filling structures) over the range of length-scales  $5$  to  $50 h^{-1} \text{ Mpc}$ . Further, it is interesting to note that we do not find any center with  $D = 1$  or  $1.5$  at this range of length-scales. This indicates the complete absence of filamentary structures at the largest range of length-scales ( $5$  to  $50 h^{-1} \text{ Mpc}$ ) that we have probed.

There is a shift to larger  $D$  values in Figure 3 as we progressively consider larger length-scales. The entire curve showing the fraction of centers as a function of  $D$  shifts to the right when we consider larger length-scales. It is quite evident from this that the nature of the structural elements that make up the Cosmic Web differs depending on the length-scale at which we view the Cosmic Web. At small scales ( $0.5 - 5 h^{-1} \text{ Mpc}$ ) we have a mixture of sheets and filaments. The fraction of sheets increases at larger length-scales ( $1 - 10 h^{-1} \text{ Mpc}$ ), whereas we predominantly have a combination of sheets and clusters at the largest length-scale ( $5 - 50 h^{-1} \text{ Mpc}$ ) that we have probed. Filaments are completely absent at the largest length-scale.

For comparison, we have also applied the Local Dimension to analyse the galaxy distribution in a semi analytic galaxy catalogue from the Millennium Simulation. We have used the semi analytic galaxy catalogue (Guo et al., 2011) to extract three different data samples with exactly

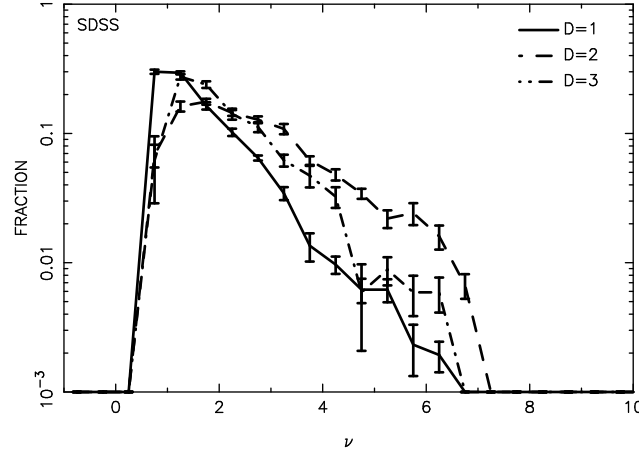


**Figure 5.** The three curves which correspond to  $D = 1, 2$  and  $3$  respectively show the fraction of galaxies as a function of  $\nu$ . The results are for the SDSS data using  $R_1 = 0.5 h^{-1} \text{ Mpc}$ ,  $R_2 = 5 h^{-1} \text{ Mpc}$  and  $R_s = 1.58 h^{-1} \text{ Mpc}$ .

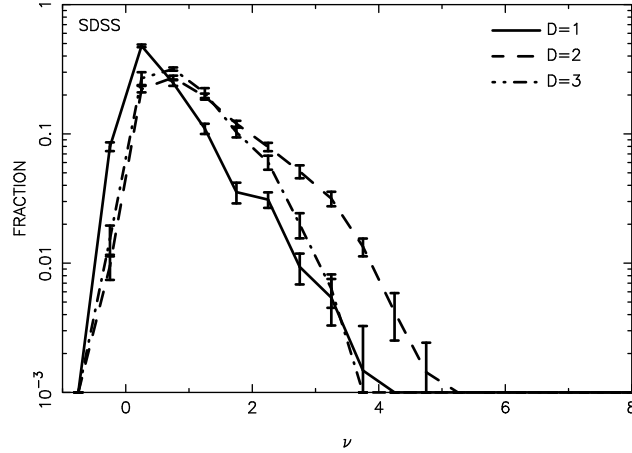


**Figure 6.** The three curves which correspond to  $D = 1, 2$  and  $3$  respectively show the fraction of galaxies as a function of  $\nu$ . The results are for the SDSS data using  $R_1 = 1 h^{-1} \text{ Mpc}$ ,  $R_2 = 10 h^{-1} \text{ Mpc}$  and  $R_s = 3.16 h^{-1} \text{ Mpc}$ .

the same geometry and galaxy number density as our SDSS sample. These three simulated data samples were analysed in exactly the same way as the actual data. The results showing the fraction of centers at different  $D$  values are presented in Figure 4. The three different curves in this figure correspond to the same range of length-scales as three different curves in Figure 3. We find that the fraction of centers with different  $D$  values have very similar distributions in the actual SDSS data and the Millennium Simulation. These curves for the SDSS data are nearly identical to those from the Millennium Simulation except for the fact that at largest length-scale ( $5 - 50 h^{-1} \text{ Mpc}$ ), the fraction of centers with  $D = 2.5$  is larger in the SDSS data as compared with the Millennium simulation. This difference in the fraction of centers lies in the  $1 - \sigma$  error-bar.

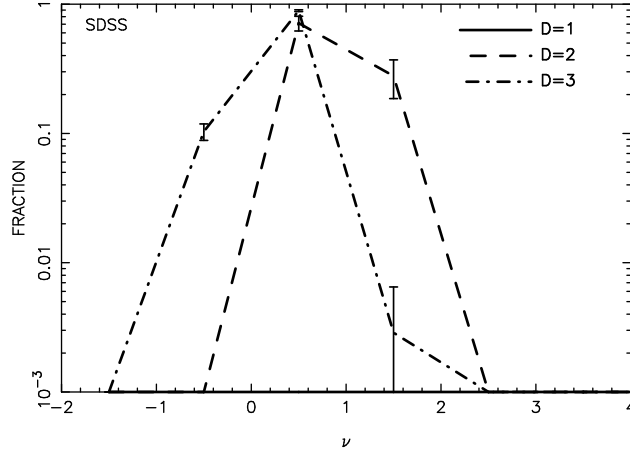


**Figure 7.** The three curves which correspond to  $D = 1, 2$  and  $3$  respectively show the fraction of galaxies as a function of  $\nu$ . The results are for the SDSS data using  $R_1 = 5 h^{-1} \text{ Mpc}$ ,  $R_2 = 50 h^{-1} \text{ Mpc}$  and  $R_s = 15 h^{-1} \text{ Mpc}$ .

## 4.2 Environment dependence

In the previous subsection, we have seen that the nature of the structural elements that make up the Cosmic Web changes depending on the length-scale at which we view the web. Our investigations show that there is a progressive transition from filaments to sheets and then clusters as we go from smaller to larger scales. In this subsection, for a fixed range of length-scales, we investigate if the distribution of a particular kind of structural element is related to the density environment. As mentioned earlier, the nature of the structural elements (*ie.*  $D$  value) depends on the range of length-scale used to determine  $D$ . The density environment too depends on the length-scale at which we smooth the density field. The length-scale range  $R_1$  to  $R_2$  used for estimating  $D$  should thus be consistent with  $R_s$ , the smoothing length-scale for the density field. In our analysis we have chosen  $R_s$  to be the geometric mean of  $R_1$  and  $R_2$  *ie.*  $R_s = \sqrt{R_1 R_2}$ . The geometric mean was chosen instead of the algebraic mean because the latter is expected to be more biased towards  $R_2$ . We expect the geometric mean to give a more representative estimate of the range of length-scales  $R_1$  to  $R_2$  which span a decade.

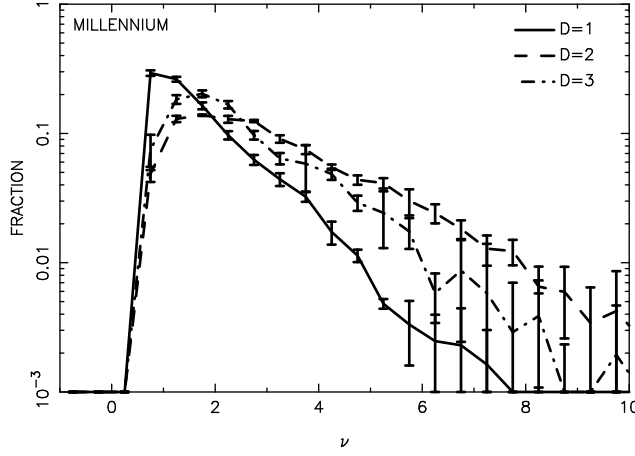
For fixed values of  $R_1$ ,  $R_2$  and  $R_s$  we focus on the distribution of the centers with a particular  $D$  value. For this purpose, the  $D$  values were divided into bins of width  $\pm 0.5$  centered at  $D = 1, 2$  and  $3$ . To determine the density environment, we have converted the entire galaxy distribution to a density field on a grid of spacing  $[0.5 h^{-1} \text{ Mpc}]^3$  using the Cloud-in-Cell method. This density field is then smoothed with a Gaussian kernel having a smoothing length  $R_s$ . The smoothing is carried out in Fourier space by multiplying the Fourier transform of the density field with  $\exp(-k^2 R_s^2/2)$  and transforming back to real space. The density field at any grid point was quantified using the dimensionless ratio  $\nu = \delta/\sigma$  where  $\delta = \delta\rho/\bar{\rho}$  is the density contrast of the smoothed density field

at the particular grid point and  $\sigma$  is the standard deviation of the density contrast of the smoothed density field evaluated using all the grid points that lie within the survey volume. Considering only the centers for which it is possible to determine a  $D$  value, we use the value of  $\nu$  at the grid point nearest to the center to assign a  $\nu$  value to each of these centers. The value of  $\nu$  associated with any of the galaxies gives an estimate of the density environment in the vicinity of the structural element centered on that galaxy.

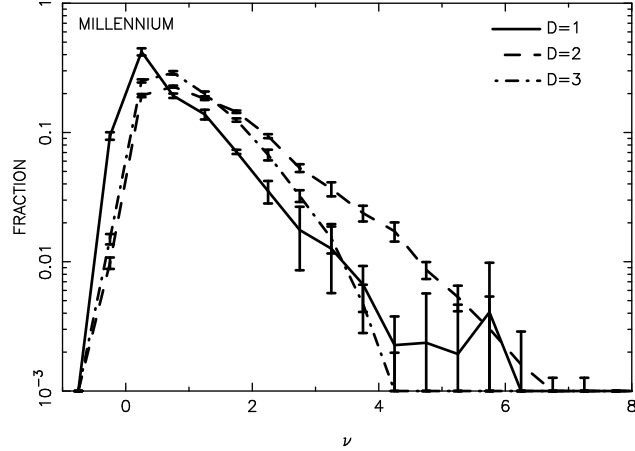
We first consider the range,  $R_1 = 0.5 h^{-1}$  Mpc and  $R_2 = 5 h^{-1}$  Mpc for which  $R_s = 1.58 h^{-1}$  Mpc and  $\sigma = 5.15$ . Figure 5 shows the results for this range of length-scales. We first consider only the centers with  $D = 1$  for which the results are shown in the solid curve of this figure. This curve shows the fraction of centers with a particular  $\nu$  value. The  $\nu$  values were divided into bins spanning  $\pm 0.25$  for this purpose. The dashed and dash-dotted curves respectively show the corresponding results for  $D = 2$  and  $3$  respectively. We find that the distribution of the fraction of centers as a function of  $\nu$  is qualitatively similar for all three values of  $D$ . The fraction shows a peak near  $\nu \sim 1$ , with a very sharp decline in the fraction at  $\nu < 1$  and a relatively gradual decline at  $\nu > 1$ . While the behaviour is qualitatively similar, there are quantitative differences between the different  $D$  values. We see that the fraction peaks at a somewhat smaller  $\nu$  value for  $D = 1$  as compared to  $D = 2$  and  $3$ . At  $\nu < 1$  the values of the fraction are somewhat larger for  $D = 1$  as compared to  $D = 2$  and  $D = 3$ . Further, the values of the fraction in the vicinity of the peak are somewhat larger for  $D = 2$  as compared to  $D = 3$ . The behaviour is reversed for  $\nu > 1$ . The fraction is smaller for  $D = 1$  in comparison to  $D = 2$  and  $3$  in the range  $1 < \nu < 3$ . For  $\nu > 3$ , we find that  $D = 3$  is roughly consistent with  $D = 1$ , whereas the fraction is considerably higher for  $D = 2$ .

Figure 6 shows the same quantities as Figure 5 with the difference that the range of length-scales now corresponds to  $R_1 = 1$  and  $R_2 = 10 h^{-1}$  Mpc for which  $R_s = 3.16 h^{-1}$  Mpc and  $\sigma = 3.09$ . The behaviour, we find, is very similar to that in Figure 5 except that the peak has shifted to a smaller  $\nu$  value ( $\nu \sim 0.5$ ). For  $\nu < 0.5$ , the fraction is larger for  $D = 1$  in comparison to  $D = 2$  and  $3$ . This is reversed for  $\nu > 0.5$  where the fraction is smaller for  $D = 1$  in comparison to  $D = 2$  and  $3$ . There is another transition around  $\nu \sim 2$ , where for  $D = 3$  the fraction falls below that of  $D = 2$ . We find that, for  $\nu > 2$ ,  $D = 1$  and  $3$  are comparable and are lower than  $D = 2$ .

Figure 7 shows the result for  $R_1 = 5$  and  $R_2 = 50 h^{-1}$  Mpc for which  $R_s = 15.8 h^{-1}$  Mpc and  $\sigma = 0.97$ . The  $\nu$  values were divided into bins spanning  $\pm 0.5$  for this purpose. The behaviour is different compared to that in Figure 5 and Figure 6. The analyse for this length-scale shows total absence of center in a filament. For  $\nu < 1.5$ , the fraction for  $D = 3$  larger in comparison to  $D = 2$ .



**Figure 8.** The three curves which correspond to  $D = 1, 2$  and  $3$  respectively show the fraction of galaxies as a function of  $\nu$ . The results are for the data from the Millennium Simulation using  $R_1 = 0.5 h^{-1} \text{ Mpc}$ ,  $R_2 = 5 h^{-1} \text{ Mpc}$  and  $R_s = 1.58 h^{-1} \text{ Mpc}$ .



**Figure 9.** The three curves which correspond to  $D = 1, 2$  and  $3$  respectively show the fraction of galaxies as a function of  $\nu$ . The results are for the data from the Millennium Simulation using  $R_1 = 1 h^{-1} \text{ Mpc}$ ,  $R_2 = 10 h^{-1} \text{ Mpc}$  and  $R_s = 3.16 h^{-1} \text{ Mpc}$ .

This situation is reverse for  $\nu > 1.5$ , where the fraction is smaller for  $D = 2$  in comparison to  $D = 3$ .

We may interpret the different curves in Figures 5 and 6 as representing the probability of finding a particular kind of structural element in the density environment corresponding to  $\nu$ . For example, the curve for  $D=1$  in Figure 5 gives the probability of finding a filament in the interval  $\nu - 0.25$  to  $\nu + 0.25$  for different values of  $\nu$ . Similarly, the curves for  $D=2$  and  $D=3$  show the probability of finding a sheet and a cluster respectively. Our analysis shows that the filaments, sheets and clusters have different probability distributions. The filaments are preferentially distributed in low density environments relative to the distribution of sheets and clusters. We have a cross-over from this behaviour at intermediate densities. The sheets are preferentially distributed relative to filaments and clusters in the high density environments. The  $\nu$  value where these transitions occur depends on our choice of  $R_1$  and  $R_2$ . For  $0.5$  to  $5 h^{-1} \text{ Mpc}$ , the density contrasts ranges are  $\nu < 1$ ,  $1 < \nu < 3$  and  $\nu > 3$  while for  $1$  to  $10 h^{-1} \text{ Mpc}$  the  $\nu$  ranges are  $\nu < 0.5$ ,  $0.5 < \nu < 2$  and

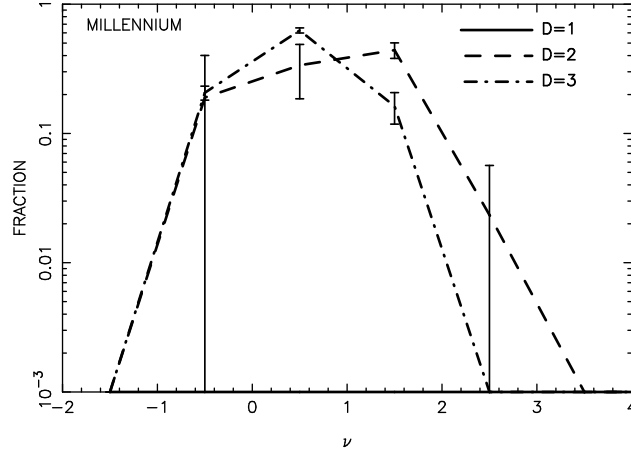


**Figure 10.** The three curves which correspond to  $D = 1, 2$  and  $3$  respectively show the fraction of galaxies as a function of  $\nu$ . The results are for the data from the Millennium Simulation using  $R_1 = 5 h^{-1} \text{ Mpc}$ ,  $R_2 = 50 h^{-1} \text{ Mpc}$  and  $R_s = 15.8 h^{-1} \text{ Mpc}$ .

$\nu > 2$ . These findings indicate that the way in which different structural elements are distributed along the Cosmic Web depends jointly on two factors (a) the local density environment, and (b) the length-scale at which we view the Cosmic Web.

For comparison, the above analysis was also performed using the galaxy distribution in the Millennium Simulation. The analysis was carried out in exactly the same way as for the actual SDSS DR7 data. The results for the Millennium simulation shown in Figures 8, 9 and 10 are analogous to the plots shown for the SDSS DR7 in Figures 5, 6 and 7 respectively. We find that the results from the Millennium Simulation are very similar to those obtained for the actual SDSS DR7 for length-scale  $0.5$  to  $5 h^{-1} \text{ Mpc}$  and  $1$  to  $10 h^{-1} \text{ Mpc}$ . The results for the length-scale  $5$  to  $50 h^{-1} \text{ Mpc}$  from Millennium Simulation differs to those obtained from the SDSS DR7. The  $\nu$  values, in Figure 10, were divided into bins spanning  $\pm 0.5$ . At  $\nu < -0.5$  the values of the fraction are somewhat similar for  $D = 2$  and  $D = 3$ . The fraction is smaller for  $D = 2$  as compared to  $D = 3$  in the range  $-0.5 < \nu < 1$ . This trend reversed for  $\nu > 1$ , where  $D = 2$  is larger compared to  $D = 3$ .

In summary the analysis of both the SDSS DR7 and the Millennium Simulation exhibit similar trends. The Local Dimensions were estimated separately in three different ranges of length-scales,  $0.5$  to  $5 h^{-1} \text{ Mpc}$ ,  $1$  to  $10 h^{-1} \text{ Mpc}$  and  $5$  to  $50 h^{-1} \text{ Mpc}$ . We find that there is a progressive shift in the  $D$  values as we move to larger length-scales. At small length-scales there is a mixtures of sheets and filaments, and the fraction of sheets increases as we move to larger length-scales ( $1$  to  $10 h^{-1} \text{ Mpc}$ ). We find that sheets and clusters are the predominant structures at the largest length-scales ( $5$  to  $50 h^{-1} \text{ Mpc}$ ). Filaments are absent at this length-scales. It is interesting to note that Forero-Romero et al. (2009) find that the mass fraction of filaments decreases while that of sheet

increases with an increase in the smoothing length-scale, which is consistent with the results of this paper.

The gradual transition, with increasing length-scales, from filaments ( $D = 1$ ) to sheets ( $D = 2$ ) and then to clusters ( $D = 3$ ) is indicative of and consistent with a transition to homogeneity ( $D = 3$ ) at large length-scales. A recent analysis of the SDSS Main galaxy sample (Sarkar et al., 2009) shows that there is transition to homogeneity at  $60 - 70 h^{-1}$  Mpc, and that the galaxy distribution is consistent with a homogeneous point distribution at length-scales larger than this. An earlier study (Pandey & Bharadwaj, 2005) had analysed thin, nearly 2-D, sections through the galaxy distribution and had found evidence for statistically significant filamentary patterns to length-scales as large as  $80 h^{-1}$  Mpc. This is apparently inconsistent with the findings of the present paper which fails to find any filaments that span across the length-scale 5 to  $50 h^{-1}$  Mpc. It should however be noted that the structures which were identified as filaments in the 2-D sections are quite likely to be sheets when the structures are viewed in full 3-D.

## ACKNOWLEDGMENT

PS would like to acknowledge Senior Research Fellowship of the University Grants Commission (UGC), India, for providing financial support during which a part of this work was done. BP acknowledges the Center for Theoretical Studies (CTS), Indian Institute of Technology, Kharagpur, for providing support to visit CTS. BP would also like to thank the Alexander von Humboldt Foundation for support through a post-doctoral fellowship.

The Millennium Simulation data bases (Lemson & Virgo Consortium, 2006) used in this paper and the web application providing online access to them were constructed as part of the activities of the German Astrophysical Virtual Observatory.

The SDSS DR7 data were downloaded from the SDSS skyserver <http://cas.sdss.org/dr7/en/>. Funding for the creation and distribution of the SDSS archive has been provided by the Alfred P. Sloan Foundation, the Participating Institutions, the National Aeronautics and Space Administration, the National Science Foundation, the US Department of Energy, the Japanese Monbukagakusho and the Max Planck Society. The SDSS web site is <http://www.sdss.org/>.

The SDSS is managed by the Astrophysical Research Consortium (ARC) for the Participating Institutions. The Participating Institutions are The University of Chicago, Fermilab, the Institute for Advanced Study, the Japan Participation Group, The Johns Hopkins University, the Korean Scientist Group, Los Alamos National Laboratory, the Max-Planck-Institute for Astronomy (MPIA),

the Max-Planck-Institute for Astrophysics (MPA), New Mexico State University, University of Pittsburgh, Princeton University, the United States Naval Observatory and the University of Washington.

## References

- Abazajian, K. N., Adelman-McCarthy, J. K., Agüeros, M. A., et al. 2009, *ApJS*, 182, 543
- Aragón-Calvo, M. A., Jones, B. J. T., van de Weygaert, R., & van der Hulst, J. M. 2007, *A&A*, 474, 315
- Aragon-Calvo, M. A., Platen, E., van de Weygaert, R., & Szalay, A. S. 2010, *ApJ*, 723, 364
- Bharadwaj S., Sahni V., Satyaprakash B. S., Shandarin S. F., & Yess C., 2000, *ApJ*, 528, 21
- Bharadwaj, S., Bhavsar, S. P., & Sheth, J. V. 2004, *ApJ*, 606, 25
- Bharadwaj, S., & Pandey, B. 2004, *ApJ*, 615, 1
- Bond J. R., Kofman L., Pogosyan D. 1996, *Nature*, 380, 603
- Bond, N. A., Strauss, M. A., & Cen, R. 2010, *MNRAS*, 409, 156
- Bruzual, G. & Charlot, S. 2003, *MNRAS*, 344, 1000
- Colless, M. et al. (for 2dFGRS team) , 2001, *MNRAS*, 328, 1039
- Colombi, S., Pogosyan, D., & Souradeep, T. 2000, *Physical Review Letters*, 85, 5515
- Croton et al. 2006, *MNRAS*, 365, 11
- De Lucia, G., & Blaizot, J. 2007, *MNRAS*, 375, 2
- El-Ad, H., & Piran, T. 1997, *ApJ*, 491, 421
- Forero-Romero, J. E., Hoffman, Y., Gottlöber, S., Klypin, A., & Yepes, G. 2009, *MNRAS*, 396, 1815
- Geller, M.J. & Huchra, J.P. 1989, *Science*, 246, 897
- Gott J. R., Mellot, A. L., & Dickinson, M. 1986, *ApJ*, 306, 341
- Guo, Q., White, S., Boylan-Kolchin, M., et al. 2011, *MNRAS*, 413, 101
- Hoyle, F., & Vogeley, M. S. 2002, *ApJ*, 566, 641
- Lemson, G., & Virgo Consortium, t. 2006, *arXiv:astro-ph/0608019*
- Mecke K. R., Buchert T. & Wagner H., 1994, *A&A*, 288, 697
- Neyrinck, M. C. 2008, *MNRAS*, 386, 2101
- Pandey, B. & Bharadwaj, S. 2005, *MNRAS*, 357, 1068
- Pandey, B., & Bharadwaj, S. 2006, *MNRAS*, 372, 827
- Pandey, B., & Bharadwaj, S. 2007, *MNRAS*, 377, L15



- Pandey, B. & Bharadwaj, S. 2008, MNRAS, 387, 767
- Pandey, B., Kulkarni, G., Bharadwaj, S., & Souradeep, T. 2011, MNRAS, 411, 332
- Platen, E., van de Weygaert, R., & Jones, B. J. T. 2007, MNRAS, 380, 551
- Sahni V., Satyaprakash B. S., & Shandarin S. F., 1998, ApJ, 495, L5
- Sarkar, P., & Bharadwaj, S. 2009, MNRAS, 394, L66
- Sarkar, P., Yadav, J., Pandey, B., & Bharadwaj, S. 2009, MNRAS, 399, L128
- Shandarin S. F., & Zeldovich I. B., 1983, Comments on Astrophysics, 10, 33
- Shectman, S. A., Landy, S. D., Oemler, A., Tucker, D. L., Lin, H., Kirshner, R. P., & Schechter, P. L. 1996, ApJ, 470, 172
- Sousbie, T., Pichon, C., Colombi, S., Novikov, D., & Pogosyan, D. 2008, MNRAS, 383, 1655
- Springel et al. 2006, Nature, 435, 629
- Stoica, R. S., Martínez, V. J., & Saar, E. 2007, Journal of the Royal Statistical Society: Series C (Applied Statistics) 56 (4), 459-477, 56, 1
- Stoughton, C., et al. 2002, AJ, 123, 485
- Strauss, M. A., et al. 2002, AJ, 124, 1810
- White S. D. M., 1979 MNRAS, 186, 145
- York, D. G., et al. 2000, AJ, 120, 1579